Mesenchymal stem cells attenuate doxorubicin-induced cellular senescence through the VEGF/Notch/TGF-β signaling pathway in H9c2 cardiomyocytes

LINGLI CHEN[1*], WENZHENG XIA[2*] and MENG HOU[3]

Departments of [1]Neurology, [2]Neurosurgery and [3]Radiation Oncology,
First Affiliated Hospital, Wenzhou Medical University, Wenzhou, Zhejiang 325000, P.R. China

Received January 4, 2018; Accepted April 5, 2018

DOI: 10.3892/ijmm.2018.3635

Abstract. The clinical use of doxorubicin (Dox) is limited by its cardiotoxicity. The fundamental changes it induces include interstitial myocardial fibrosis and the appearance of senescent cardiomyocytes. Mesenchymal stem cell (MSC)-based therapies have also been reported to modulate cellular senescence, and have been used effectively to treat age-related cardiovascular diseases. In the present study, the Transwell system was used to coculture H9c2 cells with MSCs, and their proliferation and viability were assessed. The expression of senescence-related genes p53 and p16, and telomere length were measured using reverse transcription-quantitative polymerase chain reaction analysis, and the Jagged-1/Notch-1 signaling pathway was detected using western blot analysis. The results revealed that Dox induced the senescence of H9c2 cells, characterized by a low proliferation rate, poor viability, reduced telomere length and impaired telomerase activity, and by marked increases in the expression of p53 and p16. By contrast, when cocultured with MSCs in the presence of Dox, H9c2 cell proliferation and viability increased, whereas the expression levels of p53 and p16 decreased, and telomere length and telomerase activity increased. The mechanism underlying the antisenescence function of MSCs was clarified, which involved the vascular endothelial growth factor (VEGF)/Jagged-1/Notch-1/transforming growth factor-β1 (TGF-β1) signaling pathway. It was confirmed that inhibiting VEGF, or silencing Jagged-1 or Notch-1 with small interfering RNA, or using recombinant TGF-β1 eliminated the antisenescence effects of MSCs on the Dox-treated H9c2 cells. The results revealed that MSCs rescued H9c2 cells from Dox-induced senescence through the release of VEGF, which activated the Jagged-1/Notch-1 signaling pathway, leading to the inhibition of TGF-β1 release. Therefore, treatment with MSCs may have important therapeutic implications on the attenuation of cardiotoxicity in patients with cancer treated with Dox.

Correspondence to: Dr Meng Hou, Department of Radiation Oncology, First Affiliated Hospital, Wenzhou Medical University, 2 Fuxue Lane, Wenzhou, Zhejiang 325000, P.R. China
E-mail: 244517813@qq.com

[*]Contributed equally

Key words: doxorubicin, mesenchymal stem cell, senescence, juxtacrine, vascular endothelial growth factor/Notch/transforming growth factor-β signaling pathway

Introduction

Doxorubicin (Dox) is one of the effective anthracycline anticancer drugs and is used extensively in clinical practice (1). Despite its effectiveness against cancer, its dose-dependent cardiotoxicity restricts its long-term use in chemotherapy as it reduces the quality of life of patients with cancer (2). Despite advances made over several decades, the precise mechanism underlying Dox-induced cardiomyopathy remains to be fully elucidated. Oxidative stress, inflammation and apoptosis have been suggested as the mechanisms of Dox-induced cardiotoxicity, and all these mechanisms lead to apparent cardiomyocyte senescence, which can, at least partly, result in cardiac remodeling and dysfunction (3,4). However, a specific strategy is required to protect patients against Dox-induced cardiotoxicity.

Previous studies have demonstrated that mesenchymal stem cell (MSC) transplantation attenuates myocardial damage, such as that present following myocardial infarction (5). Several studies have also shown promising results with MSC transplantation in animal models of Dox-induced heart failure (6,7). The cardioprotective effects of MSCs involve several mechanisms, including paracrine antifibrotic and anti-apoptotic factors, which may contribute to the attenuation of cardiac fibrosis following Dox treatment (6). MSCs also enhanced the capillary density, attenuating the impaired contractility of cardiomyocytes, in a model of Dox-induced heart failure (8). The mechanism underlying the protective effects of MSCs against cardiomyocyte senescence remain to be fully elucidated, although it is the main factor contributing to Dox-related cardiac remodeling and dysfunction. The present study investigated whether coculture with MSCs can

reverse the senescence of cardiomyocytes induced by Dox and the mechanism involved.

The Notch signaling pathway is an evolutionarily conserved signaling system, which regulates cell proliferation, differentiation and fate determination in embryonic and adult organs (9). Notch signaling is also involved in the self-renewal and proliferation of adult cells in several organs and cellular systems (10). Evidence has shown that the Notch ligand, Jagged-1, can be used to inhibit senescence in long-term sheet cultures of MSCs (9). Notch signaling is crucial in cardiac development, guiding the cell fate decisions that underlie myocyte and vessel differentiation (11). In cardiac progenitor cells, an increase in Notch activity reduces markers of senescence (12). Therefore, the present study examined whether modulating the Notch pathway through coculture with MSCs can relieve Dox-induced cardiac injury.

In the cardiovascular system, transforming growth factor (TGF)-β1 is involved in fibrotic cardiac remodeling (13). Dox causes dose-dependent dilated cardiomyopathy when used to treat patients with cancer, which is associated with the inhibition of endothelial cell proliferation, migration and angiogenesis by TGF-β1 (14). The TGF-β1-related apoptosis of contractile cells in the heart, cardiomyocytes, has been implicated in the cardiac damage caused by Dox (15). A previous study demonstrated that MSC transplantation improved cardiac function following myocardial infarction by inhibiting the TGF-β1/small mothers against decapentaplegic (SMAD) signaling pathway (16). Therefore, it was hypothesized that MSCs protect cardiomyocytes from Dox-related injury by inhibiting TGF-β1.

In the present study, the antisenescence effects of MSCs were investigated, and the involvement of the Jagged-1/Notch-1/TGF-β1 signaling pathway in the protection afforded by MSCs against Dox-induced cardiotoxicity was examined.

Materials and methods

Animals. Male 6-month-old Sprague-Dawley (SD) rats weighing 60-80 g were cared for in accordance with the published Guide for the Care and Use of Laboratory Animals of the United States National Institutes of Health. Rats were purchased from the Laboratory Animal Center of Wenzhou Medical University (Wenzhou, China). They were housed in a 12 h light/dark cycle at 21±2˚C, with a relative humidity of 30-70% and free access to food and water. All animal procedures were approved by the Institutional Animal Care and Use Committee of Wenzhou Medical University (Wenzhou, China).

Reagents. Dulbecco's modified Eagle's medium (DMEM) and fetal bovine serum (FBS) were obtained from HyClone Laboratories; GE Healthcare Life Sciences (Logan, UT, USA). The Transcriptor First Strand cDNA Synthesis kit, X-tremeGENE™ HP DNA transfection reagent, TeloTAGGG™ Telomerase PCR ELISAPLUS kit, and FastStart Universal SYBR Green Master (Rox) were obtained from Roche Diagnostics GmbH (Mannheim, Germany). Rabbit monoclonal antibodies directed against Notch-1 (cat. no. 3608), Jagged-1 (cat. no. 70109) and β-actin (cat. no. 4970) were purchased from Cell Signaling Technology, Inc. (Danvers, MA, USA). Notch-1 and Jagged-1 small interfering RNAs (siRNAs) were obtained from Thermo Fisher Scientific, Inc. (Waltham, MA, USA). 3-(4,5-dimethyl thiazolyl-2)-2,5-diphenyl tetrazolium bromide (MTT) and dimethyl sulfoxide (DMSO) were purchased from Sigma-Aldrich; EMD Millipore (Billerica, MA, USA). Recombinant TGF-β1 was purchased from Thermo Fisher Scientific, Inc. The Rat VEGF ELISA kit and Rat TGF-β1 ELISA kit was purchased from Abcam (Cambridge, UK).

Cell culture. Rat embryonic myoblasts (H9c2 cells) were obtained from the American Type Culture Collection (Rockville, MD, USA). The cells were cultured in DMEM supplemented with 10% FBS at 37˚C with 5% CO_2. All cells used in each assay were at passages 5-8 (17).

Bone-marrow MSCs were isolated from the femurs and tibias of the SD rats, as described previously (18). Briefly, the bone-marrow cells were flushed from the femur and tibia with 5 ml of DMEM/F12 medium. The red blood cells were lysed and discarded, and the remaining cells ($5x10^5$) were plated in a 25 cm^2 flask in 6 ml of DMEM/F12 supplemented with 10% FBS and 1% penicillin/streptomycin. The cells were cultured at 37˚C under 5% CO_2. Following 3 days in culture, the adherent MSCs were maintained in culture and the medium was replaced every 3 days. Once the culture reached 80-90% confluence, the cells were trypsinized and passaged at a dilution of 2:3. All the cells used in subsequent assays were in passages 3-5. The characteristics of the MSCs were demonstrated by immunophenotyping, as described previously (19).

Transwell cocultures of MSCs and H9c2 cells, and cell treatment. A Transwell system was used to prevent the MSCs from directly contacting the H9c2 cells. The MSCs and H9c2 cells were placed in the upper and lower chambers of the Transwell apparatus, respectively, at a density of $1x10^6$ cells/well. The H9c2 cells were pretreated with Dox (0.5 μM) for 1 h at 37˚C, as previously described (20) and, prior to coculture, they were washed with PBS. The recombinant TGF-β1 (10 ng/ml) or anti-VEGF receptor2 (anti-VEGFR2) antibody (25 μg/ml) was added to the culture medium of the H9c2 cells 1 h prior to their coculture.

Cell proliferation assay. The rate of cell proliferation was estimated with the Cell Counting Kit-8 (CCK-8) assay (HaiGene Technology, Harbin, China), according to the manufacturer's protocol. Briefly, $1x10^5$ cells were grown in a 96-well plate and incubated with the CCK-8 solution for 1 h at 37˚C, following which the absorbance of each well at 450 nm was recorded. Three replicate experiments were performed.

MTT assay. The MTT assay was used to determine cell viability. Briefly, 300 μl of MTT reagent was added to each cell-containing well 2 h prior to harvesting. The supernatant was then removed and incubated with 400 μl of DMSO for 10 min. The absorbance at 540 nm was recorded with an enzyme-linked immunosorbent assay plate reader. Three replicate experiments were performed.

Reverse transcription-quantitative polymerase chain reaction (RT-qPCR) analysis. The expression levels of several genes

Table I. Primer sequences.

Gene	Sequence
p16	F: 5'-GGTCACCGACAGGCATAACTTC-3'
p53	R: 5'-AAAGGAGGGCTGAGGCCTAA-3'
Notch-1	F: 5'-TCTGTCATCTTCCGTCCCTTCTC-3'
Jagged-1	R: 5'-CCGTGCACATAACAGACTTGGCT-3'
Telomere length	F: 5'-GATGACCTGGGCAAGTC-3'
	R: 5'-CCCTGTTGTTCTGCATATCT-3'
	F: 5'-GCTGACTTAGAATCCCTGTGTTA-3'
	R: 5'-AGGGTACTGTTGACTAGCTTT-3'
	F: 5'-GGTTTTTGAGGGTGAGGGTGAGGGTGAGGGTGA-3'
	R: 5'-TCCCGACTATCCCTATCCCTATCCCTATCCCTATCC-3'
TGF-β1	F: 5'-ATTCAAGTCAACTGTGGAGCAAC-3'
GAPDH	R: 5'-CGAAAGCCCTGTATTCCGTCT-3'
siRNA-Notch-1	F: 5'-GGCTCTCTGCTCCTCCCTGTT-3'
siRNA-Jagged-1	R: 5'-GGCTCTCTGCTCCTCCCTGTT-3'
siRNA-NT	AAG TGG GAC CTG CCT GAA TGG
	AAG GAG TAT CAG TCC CGC GTC
	AAT CGC ATA GCG TAT GCC GTT

F, forward; R, reverse; TGF-β1, transforming growth factor-β1; GAPDH, glyceraldehyde-3-phosphate dehydrogenase; siRNA, small interfering RNA; NT, scramble control.

were analyzed by RT-qPCR analysis. The expression levels of *p53, p16*, *Notch1*, Jagged-1 (*Jag1*), transforming growth factor-β1*(Tgfb1)* and *Gapdh* were analyzed, in addition to telomere length and telomerase activity. cDNA was amplified with Power SYBR Green PCR Master mix and the appropriate primers in an Applied Biosystems StepOnePlus Real-Time PCR system (Thermo Fisher Scientific, Inc.), in a reaction system of 20 μl, containing 10 μl cDNA, 4.0 μl buffer and 1 μl primers at 95˚C for 10 min, followed by 40 cycles of 15 sec at 95˚C and 1 min at 60˚C. A melting curve was generated to examine the specificity of the amplification. The relative expression levels were calculated with the $2^{-\Delta\Delta Cq}$ method (21), using *Gapdh* as the internal control. The primer pairs used to detect the mRNA levels of the target genes are listed in Table I.

Western blot analysis. Western blot analyses were performed, as previously described (18). Briefly, the cell samples were ruptured with lysis buffer. The lysates were centrifuged for 5 min at 4˚C and 12,000 x g prior to analysis of the supernatant containing the cellular proteins. Protein concentration was determined with a bicinchoninic acid protein assay kit. For each sample, 20 μg of total protein was resolved by 10% SDS-PAGE and transferred onto polyvinylidene difluoride membranes. The membranes were incubated overnight at 4˚C with antibodies directed against Notch-1, Jagged-1 and β-actin diluted at 1:1,000. The following day, the membranes were incubated for 1 h at 37˚C with horseradish peroxidase-conjugated goat anti-rabbit IgG secondary antibody (cat. no. 7074; 1:2,000; Cell Signaling Technology, Inc.), and developed with chemiluminescent substrate. The stained protein bands were visualized with the Bio-Rad ChemiDoc™ XRS system, and analyzed with the QuantityOne software (version 4.5.2; Bio-Rad Laboratories, Inc., Hercules, CA, USA).

Enzyme-linked immunosorbent assays (ELISAs). The concentrations of VEGF and TGF-β1 secreted into the cell culture media were measured with ELISA kits. The assays were performed in 96-well microplates, according to the ELISA manufacturer's protocol. Three replicate experiments were performed.

Gene knockdown with siRNA. The cells were transfected using X-tremeGENE™ HP DNA transfection reagent, according to the manufacturer's protocol. The H9c2 cells were plated in a 6-well plate at a density of $1x10^6$ cells and treated for 20 min with X-tremeGENE™ HP DNA transfection reagent at a reagent volume to siRNA mass ratio of 3:1. The cells were then transfected with the mixture containing 100 nM siRNA and incubated in 2 ml of culture medium for 48 h at 37˚C. A scrambled siRNA (siRNA-NT) was used as the control. siRNA sequences were presented in Table I. The transfection efficiencies of siRNA-Notch-1 and siRNA-Jagged-1 were assessed with RT-qPCR analysis.

Measurement of relative telomere length. The relative telomere lengths in the H9c2 cells were quantified using RT-qPCR analysis, based on a previously established method (22) and as described above. and normalized to the *Gapdh* gene. The primer pairs used to detect the telomere length are listed in Table I.

Measurement of relative telomerase activity. The telomerase activity of the H9c2 cells was examined with the TeloTAGGG™ Telomerase PCR ELISAPLUS kit, according to the manufac-

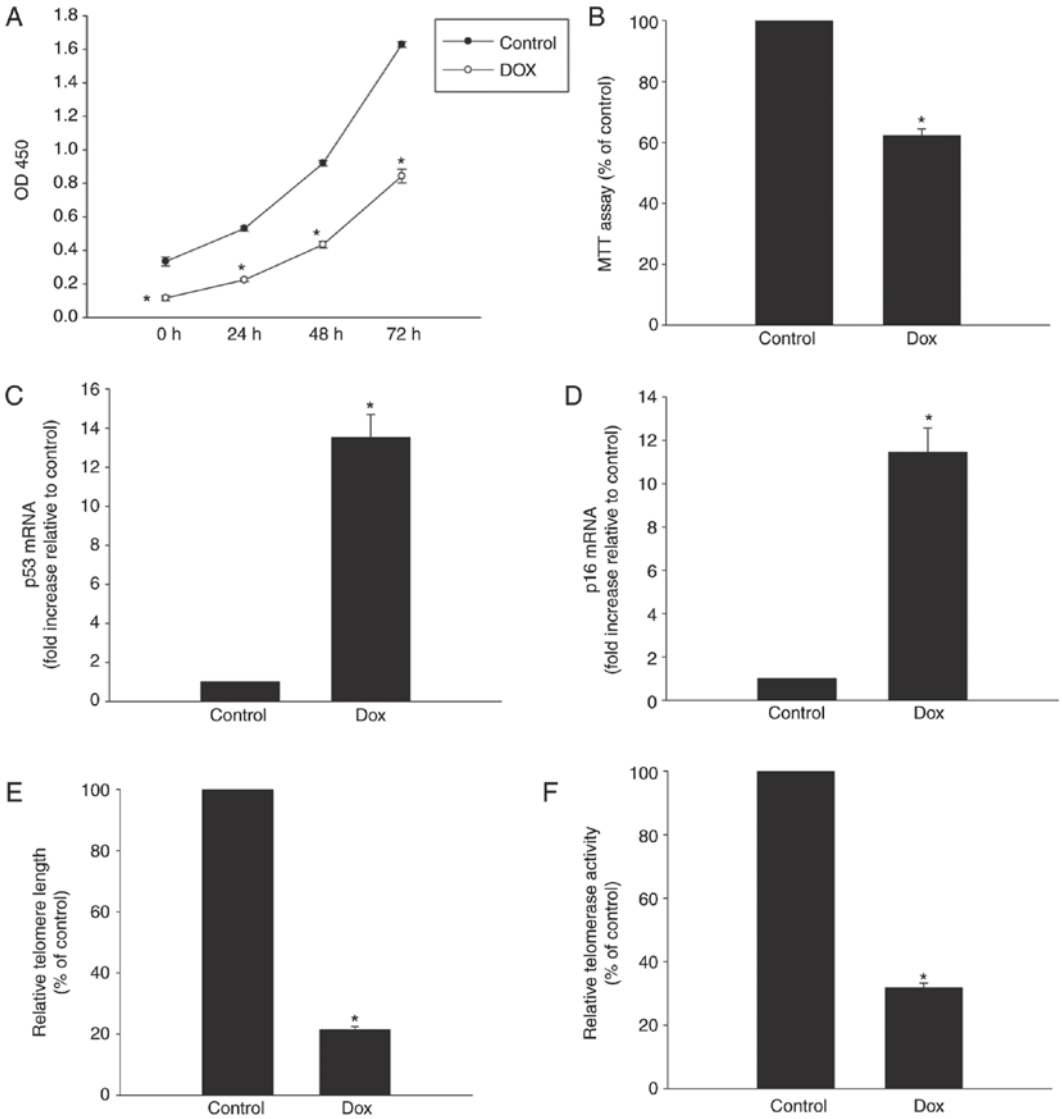

Figure 1. Dox induces the senescence of H9c2 cells. (A) Proliferation growth curves of H9c2 cells incubated with 0.5 μM Dox, determined with the Cell Counting Kit-8 proliferation assay. (B) Dox was added to the culture medium and cell viability was analyzed with an MTT assay. Reverse transcription-quantitative polymerase chain reaction analysis of mRNA levels of (C) p53, (D) p16 and (E) telomere length in H9c2 cells treated with Dox. (F) Relative telomerase activity was detected with the TeloTAGGG™ Telomerase PCR ELISAPLUS kit. Data are presented as the mean ± standard deviation of three independent experiments; *P<0.05, vs. control. Dox, doxorubicin; MTT, 3-(4,5-dimethyl thiazolyl-2)-2,5-diphenyl tetrazolium bromide.

turer's protocol. The cell lysates were centrifuged for 20 min at 4˚C and 12,000 x g, and 3 μl of cell extract was used to amplify each telomeric repeat. Inactivated cell lysate (3 μl) was used for the telomeric repeat amplification protocol (TRAP) reaction, according to the manufacturer's protocol. An internal control from the kit was amplified with each TRAP reaction to confirm the absence of any PCR inhibitor. Using ELISA, the amplified products were immobilized on streptavidin-coated microtiter plates via the biotin-streptavidin interaction, and detected with an anti-digoxigenin antibody conjugated with peroxidase for 30 min at 25˚C (100 μl working solution; included in the ELISAPLUS kit). Following the addition of a peroxidase substrate (3,3',5,5'-tetramethylbenzidine), the TRAP products were quantified by measuring the absorbance at 450 nm with a microplate reader.

Statistical analysis. Data are expressed as mean ± standard deviation. Differences among groups were compared with one-way analysis of variance followed by Tukey's multiple comparisons test, and comparisons between two groups were made with Student's t-test in the SPSS v19.0 package (IBM SPSS, Armonk, NY, USA). P<0.05 was considered to indicate a statistically significant difference.

Results

Dox induces senescence of H9c2 cells. Dox is cytotoxic towards cardiomyocytes (20), therefore, the present study investigated whether Dox induced senescence in H9c2 cells. As shown in Fig. 1A, when the H9c2 cells were treated with Dox at a concentration of 0.5 μmol/l, the proliferation rate decreased significantly immediately following treatment and remained low for at least 72 h. Dox treatment also significantly reduced the viability of the H9c2 cells, measured with the MTT assay (Fig. 1B). The expression levels of senescence-related genes p53 and p16 were markedly increased in the Dox treatment

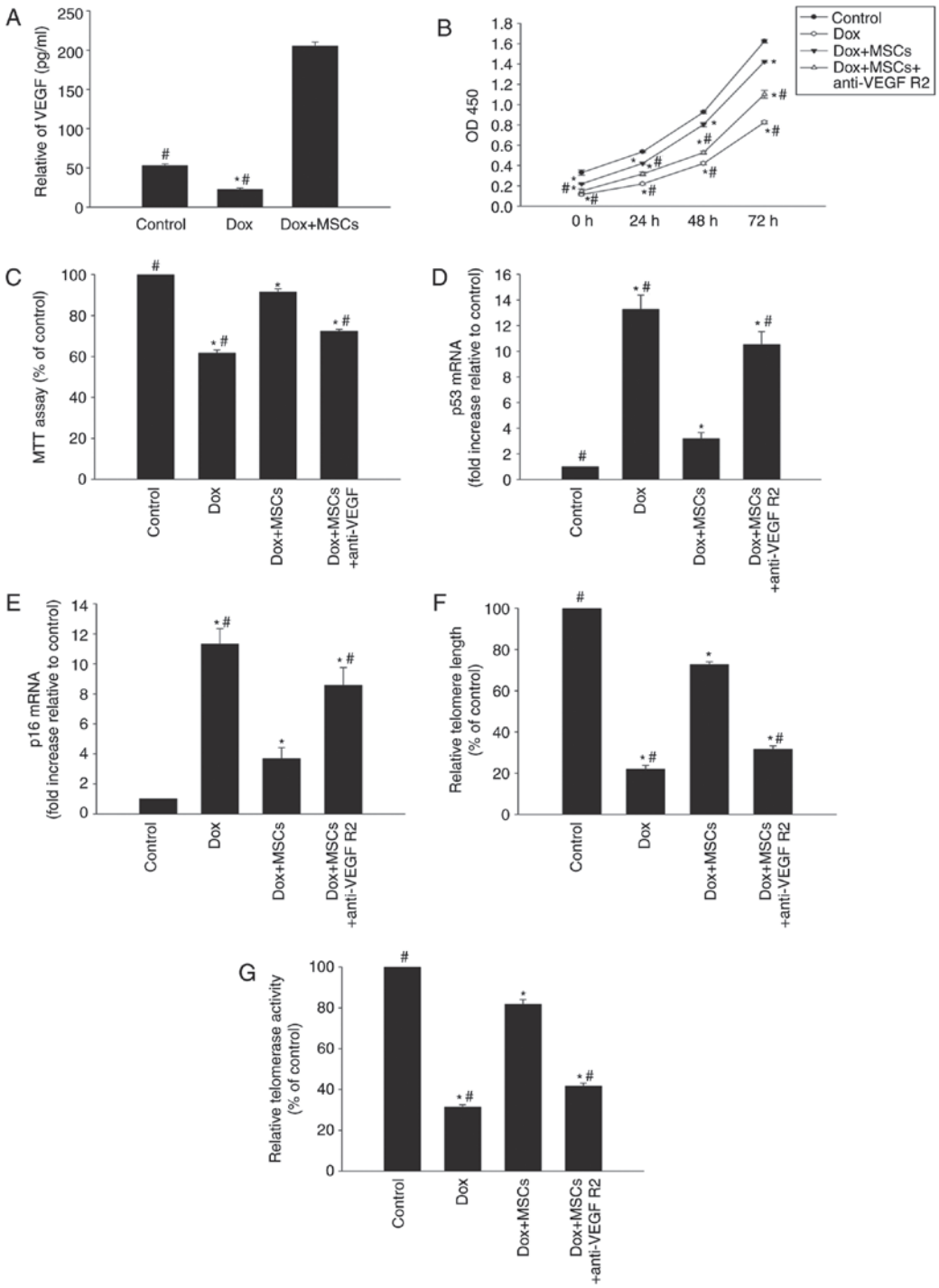

Figure 2. Coculture of cardiomyocytes with MSCs restores the cells via a VEGF juxtacrine pathway. To examine the antisenescence effects of MSCs on Dox-treated H9c2 cells, a Transwell coculture system was used. (A) ELISA of secretion of VEGF from H9c2 cells incubated with Dox or cocultured with MSCs in the presence of Dox. In H9c2 cells incubated with Dox, cocultured with MSCs in the presence of Dox, or cocultured with MSCs in the presence of Dox and anti-VEGFR2antibody, (B) cell proliferation was determined with the Cell Counting Kit-8 assay, and (C) cell viability was analyzed with the MTT assay. mRNA levels of (D) p53 and (E) p16 and (F) telomere length were analyzed with reverse transcription-quantitative polymerase chain reaction analysis. (G) Relative telomerase activity was measured. Data are presented as the mean ± standard deviation of three independent experiments; *P<0.05, vs. control; #P<0.05, vs. Dox+MSCs. Dox, doxorubicin; MSCs, mesenchymal stem cells; VEGF, vascular endothelial growth factor; VEGF R2, VEGF receptor 2; MTT, 3-(4,5-dimethyl thiazolyl-2)-2,5-diphenyl tetrazolium bromide.

group (Fig. 1C and D). Dox treatment also induced telomere shortening, which was associated with a reduction in telomerase activity (Fig. 1E and F).

Coculture with MSCs restores cardiomyocytes via the VEGF juxtacrine pathway. To examine the antisenescence effect of MSCs on Dox-treated H9c2 cells, a Transwell coculture system were used. MSCs have been shown to exert a cytoprotective effect through a juxtacrine mechanism (23), therefore, the present study examined whether MSCs restored H9c2 cells treated with Dox through a juxtacrine pathway. As expected, coculture with the MSCs induced the release of VEGF (Fig. 2A).

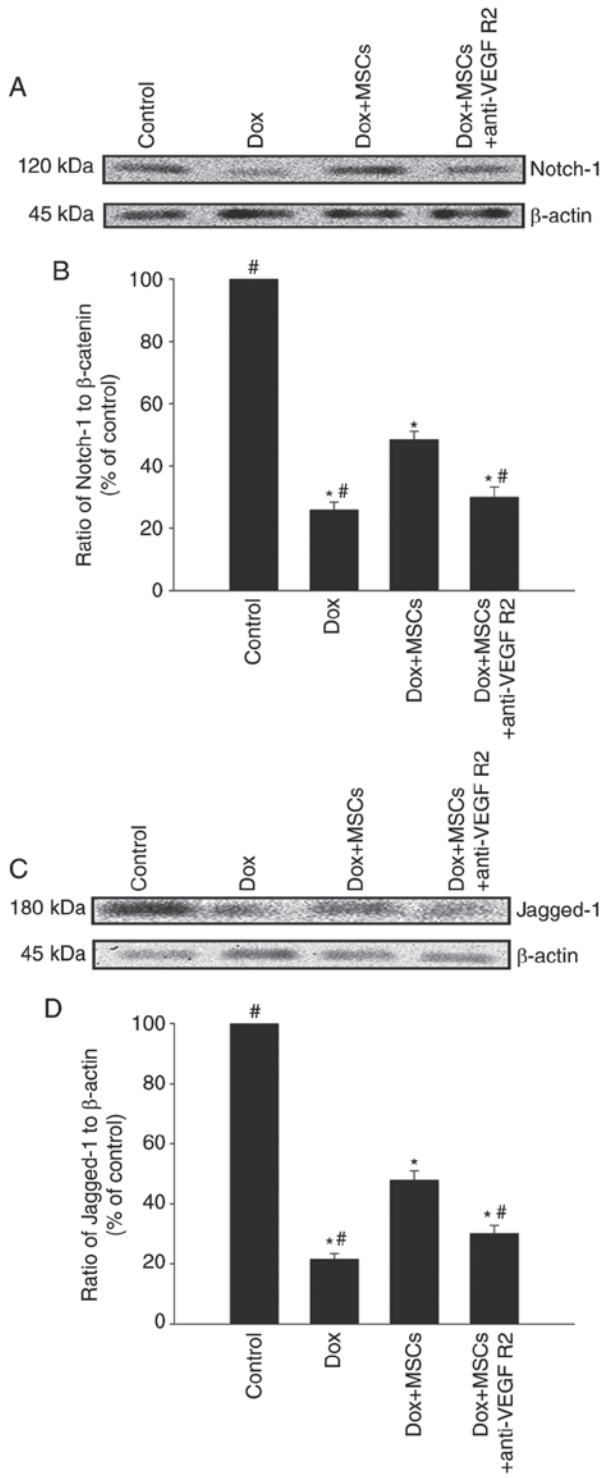

Figure 3. Coculture with MSCs activates the Jagged-1/Notch-1 signaling pathway. (A) Representative images and (B) quantification of western blot analysis of Notch-1 and β-actin. (C) Representative images and (D) quantification of western blot analysis of Jagged-1 and β-actin in H9c2 cells incubated with Dox, cocultured with MSCs in the presence of Dox, or cocultured with MSCs in the presence of Dox and anti-VEGFR2 antibody. Each column represents the mean ± standard deviation of three independent experiments; *P<0.05, vs. control; #P<0.05, vs. Dox+MSCs. Dox, doxorubicin; MSCs, mesenchymal stem cells; VEGF, vascular endothelial growth factor; VEGF R2, VEGF receptor 2.

Cell viability and proliferation were markedly higher in the Dox+MSC group, compared with that in the group treated with Dox alone (Fig. 2B and C). In addition, the expression levels of p53 and p16 were reduced in the cells exposed to Dox+MSCs, compared with their expression levels in cells treated with Dox alone (Fig. 2D and E). The addition of MSCs to the coculture system reversed the Dox-induced telomere shortening and reduced telomerase activity (Fig. 2F and G). However, the addition of anti-VEGFR2 antibody to the coculture system reversed the MSC-induced antisenescence effects (Fig. 2B-G).

Jagged-1/Notch-1 signaling pathway dynamically regulates the MSC-induced antisenescence effect. The Jagged-1/Notch-1 signaling pathway is reported to be an important regulator of rejuvenation in several cell types (24). Therefore, the present study investigated whether this pathway mediates the antisenescence effects of MSCs. As shown in Fig. 3A-D, treatment with Dox reduced the expression levels of Notch-1 and Jagged-1, which were restored by coculture with MSCs. However, when the H9c2 cells were treated with an anti-VEGFR2 antibody, the restorative effects of the MSCs were eliminated.

To confirm the role of the Jagged-1/Notch-1 pathway in the antisenescence effect of MSCs, the expression of Notch-1 or Jagged-1wassilencedwith siRNA and the senescence of H9c2 cells in the presence of Dox were examined. As shown in Fig. 4A and B, the knockdown of the *Notch1* or *Jag1* gene with siRNA reduced the expression of Notch-1 and Jagged-1respectively. Silencing *Notch1* or *Jag1* significantly attenuated the antisenescence effect of MSCs, shown by the reduced proliferation and viability of the H9c2 cells (Fig. 4C and D), and increased the expression levels of p53 and p16 (Fig. 4E and F). Silencing *Notch1* or *Jag1* also reduced the telomere length and telomerase activity in the H9c2 cells (Fig. 4G and H). By contrast, siRNA-NT had no significant effect.

Jagged-1/Notch-1 signaling pathway reciprocally regulates TGF-β1 to reverse Dox-induced senescence. TGF-β1, one of several Jagged-1/Notch-1 signaling pathway targets, is important in the cellular senescence process. In the presence of Dox, the basal mRNA expression of *Tgfb1* and the release of TGF-β1 protein from H9c2 cells were increased, whereas coculture with MSCs reduced the expression and release of TGF-β1. However, the addition of anti-VEGFR2 antibody, or the silencing of *Notch1* or *Jag1* with siRNA reduced the effects of MSCs on the expression and release of TGF-β1 (Fig. 5A and B).

Subsequently, recombinant TGF-β1 was used to examine the effect of TGF-β1. Recombinant TGF-β1 reduced H9c2 cell proliferation from day 1 of treatment, and this effect was maintained for at least 3 days. It also reduced cell viability (Fig. 5C and D), compared with that in the cells cocultured with MSCs only. Recombinant TGF-β1 also rescued the previously observed reduction in p53 and p16 caused by coculture with MSCs (Fig. 5E and F), and eliminated the antisenescence effects of MSCs on telomere length and activity (Fig. 5G and H).

Discussion

Dox is one of the most widely used chemotherapeutic agents and is effective against a wide range of tumors (25). Despite its beneficial effects against cancer, the clinical use of Dox

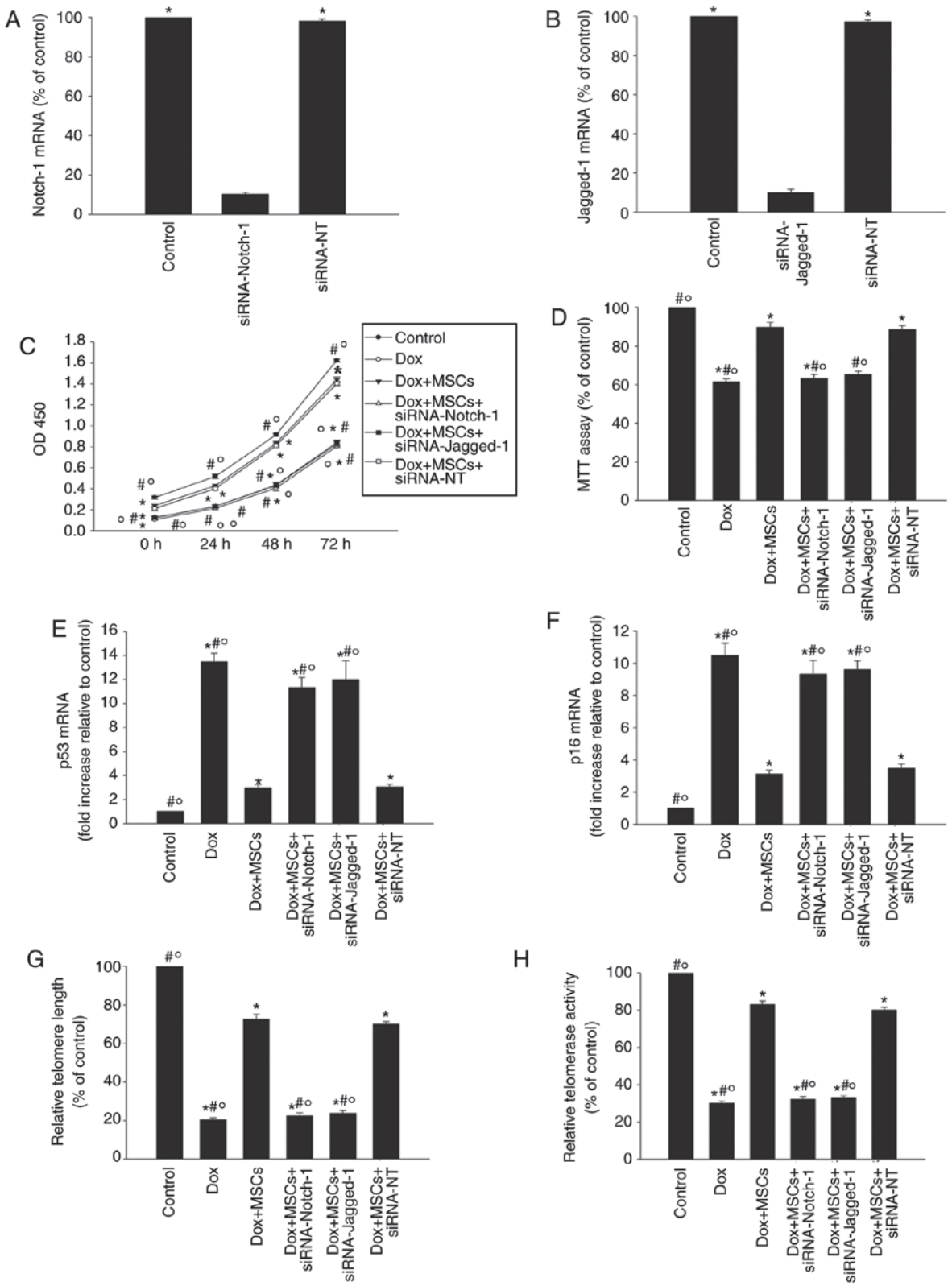

Figure 4. Jagged-1/Notch-1 signaling pathway dynamically regulates MSC antisenescence effects. (A) H9c2 cells were transfected with siRNA directed against Notch-1 or with siRNA-NT as the control. siRNA-mediated transfection efficiency was determined with RT-qPCR. Each column represents the mean ± standard deviation of three independent experiments; *P<0.05, vs. siRNA-Notch-1. (B) H9c2 cells were transfected with siRNA directed against Jagged-1 or with siRNA-NT as the control. siRNA-mediated transfection efficiency was determined with RT-qPCR. Each column represents the mean ± standard deviation of three independent experiments; *P<0.05, vs. siRNA-Jagged-1. To determine whether the Jagged-1/Notch-1 signaling pathway is involved in the antisenescence actions of MSCs, H9c2 cells were transfected with siRNA against Notch-1 or Jagged-1, or with siRNA-NT as the control, and then cocultured with MSCs in the presence of Dox. In parallel experiments, the cells were treated with Dox alone or cocultured with MSCs in the presence of Dox. H9c2 cells under normal culture conditions were used as the control. (C) Growth (proliferation) curves of H9c2 cells determined with a Cell Counting Kit-8 assay. (D) Cellular viability was analyzed with an MTT assay. (E) p53, (F) p16 and (G) telomere length were analyzed with RT-qPCR analysis. (H) Relative telomerase activity was measured. Data are presented as the mean ± standard deviation of three independent experiments; *P<0.05, vs. control; #P<0.05, vs. Dox+MSCs; °P<0.05, vs. Dox+MSCs+siRNA-NT. Dox, doxorubicin; MSCs, mesenchymal stem cells; siRNA, small interfering RNA; NT, scramble control; MTT, 3-(4,5-dimethyl thiazolyl-2)-2,5-diphenyl tetrazolium bromide; RT-qPCR, reverse transcription-quantitative polymerase chain reaction.

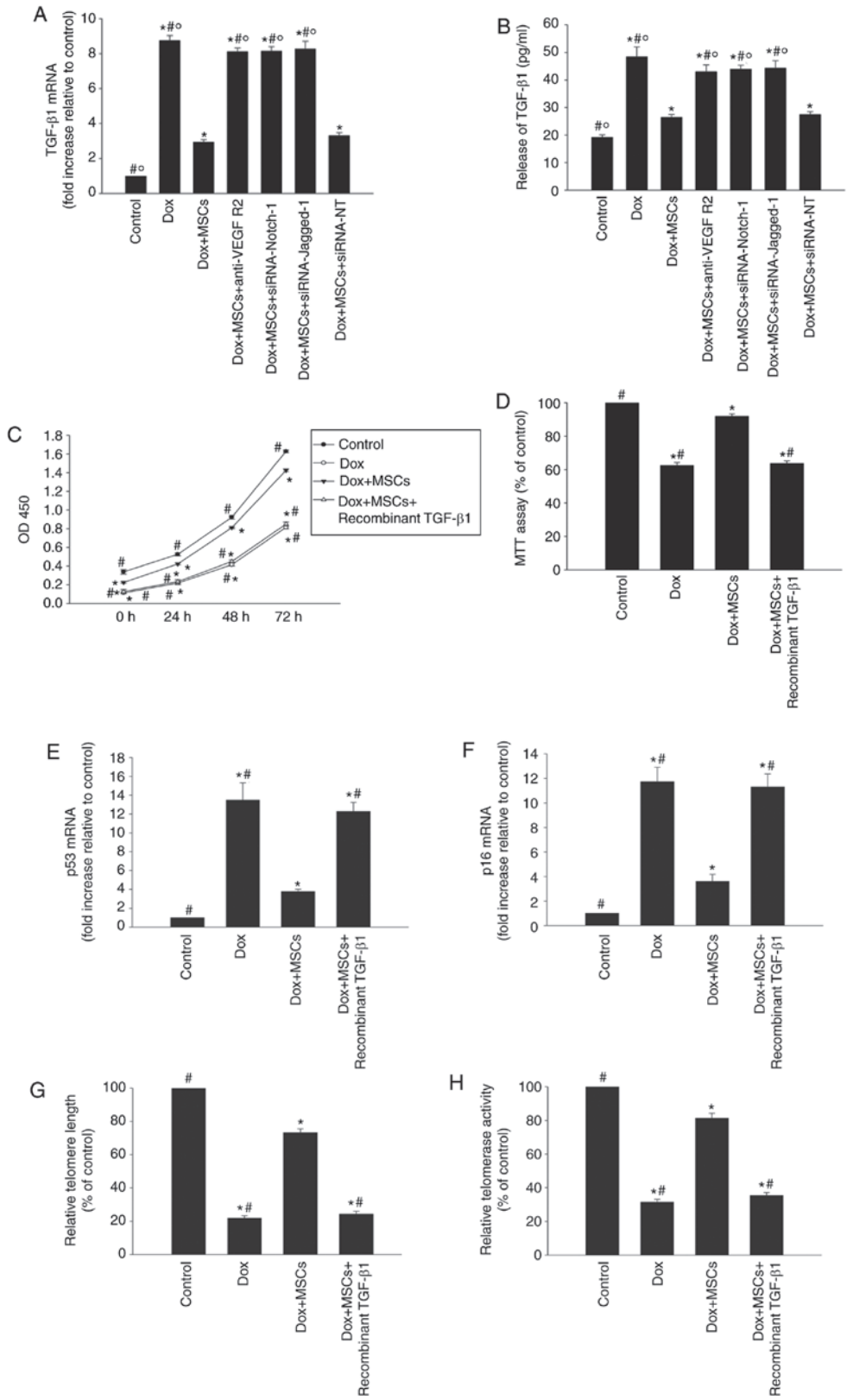

Figure 5. Jagged-1/Notch-1 signaling pathway reciprocally regulates TGF-β1 to reverse Dox-induced senescence. H9c2 cells were transfected with siRNA directed against Notch-1 or Jagged-1, or with siRNA-NT as the control, and then cocultured with MSCs in the presence of Dox. In parallel experiments, H9c2 cells were incubated with Dox, cocultured with MSCs in the presence of Dox, or cocultured with MSCs in the presence of Dox and anti-VEGFR2 antibody. H9c2 cells under normal culture conditions were used as the control. (A) RT-qPCR analysis of mRNA levels of TGF-β1. (B) Concentrations of TGF-β1 in the culture medium were analyzed with an enzyme-linked immunosorbent assay. Each column represents the mean ± standard deviation of three independent experiments; *P<0.05, vs. control; $^{\#}$P<0.05, vs. Dox+MSCs; $^{\circ}$P<0.05, vs. Dox+MSCs+siRNA-NT. In H9c2 cells incubated with Dox, cocultured with MSCs in the presence of Dox, or cocultured with MSCs in the presence of Dox and recombinant TGF-β1, (C) cell proliferation was determined with the Cell Counting Kit-8 assay, and (D) viability was analyzed with an MTT assay. (E) p53, (F) p16 and (G) telomere length were analyzed with RT-qPCR analysis. (H) Relative telomerase activity was measured. Data are presented as the mean ± standard deviation of three independent experiments; *P<0.05, vs. Dox; $^{\#}$P<0.05, vs. Dox+MSCs+recombinant TGF-β1. Dox, doxorubicin; MSCs, mesenchymal stem cells; TGF-β1, transforming growth factor-β1; siRNA, small interfering RNA; NT, scramble control; MTT, 3-(4,5-dimethyl thiazolyl-2)-2,5-diphenyl tetrazolium bromide; RT-qPCR, reverse transcription-quantitative polymerase chain reaction.

has the serious disadvantage of cardiotoxicity, which seriously limits its oncological therapeutic applicability (26). The mechanism of Dox-induced cardiotoxicity has been investigated extensively but remains controversial, although cellular senescence is considered to be a possible important mechanism (27). Modulating cellular senescence may allow the development of cardioprotective strategies, avoid the interruption or discontinuation of necessary cancer treatments, and reduce early and late cardiovascular and oncological morbidity and mortality rates (28,29). The data in the present study suggested that Dox-induced cardiotoxicity developed from the specific accumulation of cellular senescence, accompanied by the elevated expression of senescence-related genes, reduced telomere length and reduced telomerase activity.

Previous studies have reported that the administration of autologous bone-marrow-derived MSCs improves the left ventricular ejection fraction and other cardiac functional parameters in models of Dox-induced dilated cardiomyopathy (30). However, the mechanism of this therapeutic approach remains to be fully elucidated. MSCs have previously been shown to significantly reduce ischemic cardiac damage through a paracrine pathway (31) and, in a previous study, the culture medium of MSCs antagonized the senescence and apoptosis of cardiomyocytes and cardiac progenitor cells, two major processes in Dox-induced cardiotoxicity (32). The results of the present study suggested that MSCs exert an antisenescence effect by triggering the secretion of VEGF, and that this effect is reduced by an anti-VEGFR2 antibody. Asa previous study found that H9c2 cells also express VEGF (33), the present study used RT-qPCR analysis to examine the mRNA level of VEGF in the H9c2 cells, however the results of the RT-qPCR analysis showed no difference between the H9c2 cells cocultured with MSCs and H9c2 cells alone. The increase of free VEGF in the H9c2 MSC coculture may result from the MSCs only.

Unlike several other agonist/receptor systems, Notch signaling relies on non-diffusible ligands (δ, δ-like, and Jagged), which are integral membrane proteins that engage with and activate the surface receptors on immediately adjacent cells (9). Notch is involved in embryonic development, cell fate determination and cancer. It has also been linked to senescence; in oxygen-tension-regulated self-renewal, the Notch signaling pathway was activated in MSCs (34). The Notch signaling pathway is closely associated with Dox-induced cardiac injury, and a previous study detected an initial reduction in the expression of Notch pathway genes on day 3 following Dox treatment, corresponding to cardiomyocyte death by apoptosis and necrosis (35). The data from the present study showed that the Jagged-1/Notch-1 signaling pathway was significantly inhibited when the H9c2 cells were treated with Dox, whereas coculture with MSCs activated the Jagged-1/Notch-1 signaling pathway, exerting a restorative effect, which was eliminated by silencing of the *Notch1* or *Jag1* gene.

Numerous compounds with prosenescence effects have been assessed in models of Dox-induced cardiotoxicity. TGF-β is associated with Dox-induced cardiotoxicity (36). In the cardiovascular system, TGF-β is involved in fibrotic cardiac remodeling, and a previous study suggested that inhibition of the TGF-β pathway alleviates left ventricular remodeling and systolic and diastolic dysfunction, thus alleviating the detrimental effects of Dox on endothelial cells (37). It has also been demonstrated that the inhibition of TGF-β attenuates diastolic dysfunction by reducing cardiac fibrosis in a model of anthracycline-induced cardiomyopathy (38). A previous study indicated that TGF-β can induce cellular senescence through repressing the telomerase reverse transcriptase gene in tumor cells (39), coincident with the results in the present study, in which Dox induced the elevation of TGF-β, leading to shortening telomere length and impairing the telomerase activity. MSC transplantation has been shown to significantly inhibit cardiac fibrosis following myocardial infarction and mediate a reduction in the expression of TGF-β/SMAD2 (40). In the present study, increased expression of TGF-β was detected in the Dox-treated H9c2 cells, which was reduced by coculture of the cells with MSCs. It was found that recombinant TGF-β1 decreased the antisenescence effects of the MSCs.

In conclusion, the present study demonstrated that the attenuation of cardiomyocyte senescence during coculture with MSCs may have important therapeutic implications for Dox-induced cardiomyopathy. The results of the present study suggested that MSCs protected H9c2 cells from Dox-induced senescence by stimulating the secretion of VEGF, leading to activation of the Notch-1/Jagged-1 signaling pathway, which then inhibited the secretion of TGF-β1. The coculture of cardiomyocytes with MSCs may provide a unique therapeutic opportunity targeting cell senescence, in a useful strategy for the treatment of Dox-induced cardiomyopathy.

Acknowledgements

Not applicable.

Funding

This study was supported by the National Natural Science Foundation of China (grant nos. 81600278 and 81500261 to WZX and MH, respectively) and the Medical Science and Technology Project of Zhejiang Province (grant no. 2018KY517 to MH).

Availability of data and materials

All data generated or analyzed during the present study are included in the published article.

Authors' contributions

LC and WX made substantial contributions to the acquisition of data, analysis and interpretation of data. MH was involved in conception and design of the study, drafting the manuscript and revising it critically for important intellectual content.

Ethics approval and consent to participate

All animal procedures were approved by the Institutional Animal Care and Use Committee of Wenzhou Medical University.

Consent for publication

Not applicable.

Competing interests

The authors declare that they have no competing interests.

References

1. Octavia Y, Tocchetti CG, Gabrielson KL, Janssens S, Crijns HJ and Moens AL: Doxorubicin-induced cardiomyopathy: From molecular mechanisms to therapeutic strategies. J Mol Cell Cardiol 52: 1213-1225, 2012.
2. Carvalho C, Santos RX, Cardoso S, Correia S, Oliveira PJ, Santos MS and Moreira PI: Doxorubicin: The good, the bad and the ugly effect. Curr Med Chem 16: 3267-3285, 2009.
3. Stěrba M, Popelová O, Vávrová A, Jirkovský E, Kovaříková P, Geršl V and Simůnek T: Oxidative stress, redox signaling, and metal chelation in anthracycline cardiotoxicity and pharmacological cardioprotection. Antioxid Redox Signal 18: 899-929, 2013.
4. Singh P, Sharma R, McElhanon K, Allen CD, Megyesi JK, Beneš H and Singh SP: Sulforaphane protects the heart from doxorubicin-induced toxicity. Free Radic Biol Med 86: 90-101, 2015.
5. Guarita-Souza LC, Teixeira de Carvalho KA, Francisco JC, Simeoni R and Faria-Neto JR: Cellular transplantation for the treatment of non-ischaemic dilated cardiomyopathies. Eur Heart J Suppl 10: K7-K10, 2008.
6. Mohammadi Gorji S, Karimpor Malekshah AA, Hashemi-Soteh MB, Rafiei A, Parivar K and Aghdami N: Effect of mesenchymal stem cells on doxorubicin-induced fibrosis. Cell J 14: 142-151, 2012.
7. Ezquer F, Gutiérrez J, Ezquer M, Caglevic C, Salgado HC and Calligaris SD: Mesenchymal stem cell therapy for doxorubicin cardiomyopathy: Hopes and fears. Stem Cell Res Ther 6: 116, 2015.
8. Garbade J, Dhein S, Lipinski C, Aupperle H, Arsalan M, Borger MA, Barten MJ, Lehmann S, Walther T and Mohr FW: Bone marrow-derived stem cells attenuate impaired contractility and enhance capillary density in a rabbit model of doxorubicin-induced failing hearts. J Card Surg 24: 591-599, 2009.
9. Tian Y, Xu Y, Xue T, Chen L, Shi B, Shu B, Xie C, Max Morandi M, Jaeblon T, Marymont JV and Dong Y: Notch activation enhances mesenchymal stem cell sheet osteogenic potential by inhibition of cellular senescence. Cell Death Dis 8: e2595, 2017.
10. Iglesias-Bartolome R and Gutkind JS: Signaling circuitries controlling stem cell fate: To be or not to be. Curr Opin Cell Biol 23: 716-723, 2011.
11. Towbin JA, Lorts A and Jefferies JL: Left ventricular non-compaction cardiomyopathy. Lancet 386: 813-825, 2015.
12. Gude N, Joyo E, Toko H, Quijada P, Villanueva M, Hariharan N, Sacchi V, Truffa S, Joyo A, Voelkers M, *et al*: Notch activation enhances lineage commitment and protective signaling in cardiac progenitor cells. Basic Res Cardiol 110: 29, 2015.
13. Ieronimakis N, Hays AL, Janebodin K, Mahoney WM Jr, Duffield JS, Majesky MW and Reyes M: Coronary adventitial cells are linked to perivascular cardiac fibrosis via TGFβ1 signaling in the mdx mouse model of duchenne muscular dystrophy. J Mol Cell Cardiol 63: 122-134, 2013.
14. Castañares C, Redondo-Horcajo M, Magán-Marchal N, Ten Dijke P, Lamas S and Rodríguez-Pascual F: Signaling by ALK5 mediates TGF-beta-induced ET-1 expression in endothelial cells: A role for migration and proliferation. J Cell Sci 120: 1256-1266, 2007.
15. Konorev EA, Vanamala S and Kalyanaraman B: Differences in doxorubicin-induced apoptotic signaling in adult and immature cardiomyocytes. Free Radic Biol Med 45: 1723-1728, 2008.
16. Hou J, Wang L, Hou J, Guo T, Xing Y, Zheng S, Zhou C, Huang H, Long H, Zhong T, *et al*: Peroxisome proliferator-activated receptor gamma promotes mesenchymal stem cells to express connexin43 via the inhibition of tgf-β1/smads signaling in a rat model of myocardial infarction. Stem Cell Rev 11: 885-899, 2015.
17. Witek P, Korga A, Burdan F, Ostrowska M, Nosowska B, Iwan M and Dudka J: The effect of a number of H9C2 rat cardiomyocytes passage on repeatability of cytotoxicity study results. Cytotechnology 68: 2407-2415, 2016.
18. Xia W, Zhang F, Xie C, Jiang M and Hou M: Macrophage migration inhibitory factor confers resistance to senescence through cd74-dependent ampk-foxo3a signaling in mesenchymal stem cells. Stem Cell Res Ther 6: 82, 2015.
19. Hou M, Liu J, Liu F, Liu K and Yu B: C1q tumor necrosis factor-related protein-3 protects mesenchymal stem cells against hypoxia- and serum deprivation-induced apoptosis through the phosphoinositide 3-kinase/Akt pathway. Int J Mol Med 33: 97-104, 2014.
20. Piegari E, Russo R, Cappetta D, Esposito G, Urbanek K, Dell'Aversana C, Altucci L, Berrino L, Rossi F and De Angelis A: MicroRNA-34a regulates doxorubicin-induced cardiotoxicity in rat. Oncotarget 7: 62312-62326, 2016.
21. Livak KJ and Schmittgen TD: Analysis of relative gene expression data using real-time quantitative PCR and the 2-(Delta Delta C(T)) method. Methods 25: 402-408, 2001.
22. Xia W and Hou M: Macrophage migration inhibitory factor rescues mesenchymal stem cells from doxorubicin-induced senescence though the PI3K-Akt signaling pathway. Int J Mol Med 41: 1127-1137, 2018.
23. Kourembanas S: Exosomes: Vehicles of intercellular signaling, biomarkers, and vectors of cell therapy. Annu Rev Physiol 77: 13-27, 2015.
24. Xu LL, Fu HX, Zhang JM, Feng FE, Wang QM, Zhu XL, Xue J, Wang CC, Chen Q, Liu X, *et al*: Impaired function of bone marrow mesenchymal stem cells from immune thrombocytopenia patients in inducing regulatory dendritic cell differentiation through the Notch-1/Jagged-1 signaling pathway. Stem Cell Dev 26: 1648-1661, 2017.
25. Cardinale D, Colombo A, Bacchiani G, Tedeschi I, Meroni CA, Veglia F, Civelli M, Lamantia G, Colombo N, Curigliano G, *et al*: Early detection of anthracycline cardiotoxicity and improvement with heart failure therapy. Circulation 131: 1981-1988, 2015.
26. Carver JR, Shapiro CL, Ng A, Jacobs L, Schwartz C, Virgo KS, Hagerty KL, Somerfield MR, Vaughn DJ and ASCO Cancer Survivorship Expert Panel: American society of clinical oncology clinical evidence review on the ongoing care of adult cancer survivors: Cardiac and pulmonary late effects. J Clin Oncol 25: 3991-4008, 2007.
27. Du WW, Yang W, Chen Y, Wu ZK, Foster FS, Yang Z, Li X and Yang BB: Foxo3 circular RNA promotes cardiac senescence by modulating multiple factors associated with stress and senescence responses. Eur Heart J 38: 1402-1412, 2017.
28. Jackson JG, Pant V, Li Q, Chang LL, Quintás-Cardama A, Garza D, Tavana O, Yang P, Manshouri T, Li Y, *et al*: p53-mediated senescence impairs the apoptotic response to chemotherapy and clinical outcome in breast cancer. Cancer Cell 21: 793-806, 2012.
29. Baar MP, Brandt RMC, Putavet DA, Klein JDD, Derks KWJ, Bourgeois BRM, Stryeck S, Rijksen Y, van Willigenburg H, Feijtel DA, *et al*: Targeted apoptosis of senescent cells restores tissue homeostasis in response to chemotoxicity and aging. Cell 169: 132-147, 2017.
30. Mao C, Hou X, Wang B, Chi J, Jiang Y, Zhang C and Li Z: Intramuscular injection of human umbilical cord-derived mesenchymal stem cells improves cardiac function in dilated cardiomyopathy rats. Stem Cell Res Ther 8: 18, 2017.
31. Bollini S, Cheung KK, Riegler J, Dong X, Smart N, Ghionzoli M, Loukogeorgakis SP, Maghsoudlou P, Dubé KN, Riley PR, *et al*: amniotic fluid stem cells are cardioprotective following acute myocardial infarction. Stem Cells Dev 20: 1985-1994, 2011.
32. Lazzarini E, Balbi C, Altieri P, Pfeffer U, Gambini E, Canepa M, Varesio L, Bosco MC, Coviello D, Pompilio G, *et al*: The human amniotic fluid stem cell secretome effectively counteracts doxorubicin-induced cardiotoxicity. Sci Rep 6: 29994, 2016.
33. Zhou N, Fu Y, Wang Y, Chen P, Meng H, Guo S, Zhang M, Yang Z and Ge Y: p27kip1 haplo-insufficiency improves cardiac function in early-stages of myocardial infarction by protecting myocardium and increasing angiogenesis by promoting IKK activation. Sci Rep 4: 5978, 2014.
34. Rios C, D'Ippolito G, Curtis KM, Delcroix GJ, Gomez LA, El Hokayem J, Rieger M, Parrondo R, de Las Pozas A, Perez-Stable C, *et al*: Low oxygen modulates multiple signaling pathways increasing self-renewal while decreasing differentiation, senescence and apoptosis in stromal miami cells. Stem Cells Dev 25: 848-460, 2016.
35. Packard RRS, Baek KI, Beebe T, Jen N, Ding Y, Shi F, Fei P, Kang BJ, Chen PH, Gau J, *et al*: Automated segmentation of light-sheet fluorescent imaging to characterize experimental doxorubicin-induced cardiac injury and repair. Sci Rep 7: 8603, 2017.

36. Chua S, Lee FY, Chiang HJ, Chen KH, Lu HI, Chen YT, Yang CC, Lin KC, Chen YL, Kao GS, *et al:* The cardioprotective effect of melatonin and exendin-4 treatment in a rat model of cardiorenal syndrome. J Pineal Res 61: 438-456, 2016.
37. Sun Z, Schriewer J, Tang M, Marlin J, Taylor F, Shohet RV and Konorev EA: The TGF-β pathway mediates doxorubicin effects on cardiac endothelial cells. J Mol Cell Cardiol 90: 129-138, 2016.
38. Cappetta D, Esposito G, Piegari E, Russo R, Ciuffreda LP, Rivellino A, Berrino L, Rossi F, De Angelis A and Urbanek K: SIRT1 activation attenuates diastolic dysfunction by reducing cardiac fibrosis in a model of anthracycline cardiomyopathy. Int J Cardiol 205: 99-110, 2016.
39. Li H, Xu D, Toh BH and Liu JP: TGF-beta and cancer: Is Smad3 a repressor of hTERT gene? Cell Res 16: 169-173, 2006.
40. Chen P, Wu R, Zhu W, Jiang Z, Xu Y, Chen H, Zhang Z, Chen H, Zhang L, Yu H, *et al*: Hypoxia preconditioned mesenchymal stem cells prevent cardiac fibroblast activation and collagen production via leptin. PloS one 9: e103587, 2014.